FULL PAPER

Improved Functionality of Lithium-Ion Batteries Enabled by Atomic Layer Deposition on the Porous Microstructure of Polymer Separators and Coating Electrodes

Yoon Seok Jung, Andrew S. Cavanagh, Lynn Gedvilas, Nicodemus E. Widjonarko, Isaac D. Scott, Se-Hee Lee, Gi-Heon Kim, Steven M. George, and Anne C. Dillon**

Atomic layer deposition (ALD) of Al_2O_3 is applied on a polypropylene separator for lithium-ion batteries. A thin Al_2O_3 layer (<10 nm) is coated on every surface of the porous polymer microframework without significantly increasing the total separator thickness. The thin Al_2O_3 ALD coating results in significantly suppressed thermal shrinkage, which may lead to improved safety of the batteries. More importantly, the wettability of Al_2O_3 ALD-coated separators in an extremely polar electrolyte based on pure propylene carbonate (PC) solvent is demonstrated, without any decrease in electrochemical performances such as capacity, rate capability, and cycle life. Finally, a $LiCoO_2$/natural graphite full cell is demonstrated under extremely severe conditions (pure PC-based electrolyte and high (4.5 V) upper cut-off potential), which is enabled by the Al_2O_3 ALD coating on all three components (cathode, anode, and separator).

1. Introduction

Development of high-performance lithium-ion batteries (LIBs) is becoming a high priority for the replacement of conventional gasoline-fueled vehicles by fully electric vehicles and/or plug-in hybrid electric vehicles.[1–3] Extensive research has been performed to develop improved LIB electrodes, however, very little has been carried out to improve separator technologies even though they are critical to the performance of LIBs, especially for high power and safety.[4] Commercial separators for LIBs are typically porous polyolefin (polyethylene [PE] and polypropylene [PP]) films with thicknesses of ≤25 μm. Although the separators are generally reliable for portable applications, it is critical that two major limitations are overcome for vehicular storage. First, the polymer separators shrink and melt at elevated temperatures.[4] For example, if the temperature in a battery increases because of an internal short circuit (ISC), shrinking/melting may occur. This may increase propagation of an ISC, generating excessive Joule heating that causes undesirable exothermic electrode side reactions, often leading to catastrophic thermal runaway.[5] Second, the polymer separators are not compatible with some conventional electrolytes that include solvents of high dielectric constants (e.g., propylene carbonate [PC] and ethylene carbonate [EC]), due to hydrophobicity and low surface energies of the polyolefins, which cause wetting problems.[4] In a LIB manufacturing process, after a prerolled or prestacked thin-layered porous electrode assembly is placed inside a LIB cell container, a liquid electrolyte is then injected. Because the metal current collectors are foils, transport of the liquid electrolyte occurs in a highly directional manner through the thin porous channel formed by the electrode materials and separator. The wettability issue becomes more critical for large-capacity electrodes being developed for vehicular applications where the entrance area is limited, and the transport distance increases for the electrolyte.

To solve the poor wettability problem of conventional polymer separators, various surface modification approaches have been tried, such as polymer coatings[6–8] and a polydopamine treatment.[9] As approaches to overcome thermal shrinkage, inorganic–polymer composite films[10,11] or inorganic/polymer/inorganic trilayer films[12–15] have been fabricated. The introduction of inorganic components can enhance the wettability of the electrolyte. However, further improvement is still warranted for

Dr. Y. S. Jung, Dr. L. Gedvilas, N. E. Widjonarko, I. D. Scott, Dr. G.-H. Kim, Dr. A. C. Dillon
National Renewable Energy Laboratory
Golden, CO 80401, USA
E-mail: ysjung@unist.ac.kr; Anne.Dillon@nrel.gov
Prof. Y. S. Jung
Interdisciplinary School of Green Energy
Ulsan National Institute of Science and Technology (UNIST)
Ulsan 689-798, Republic of Korea
I. D. Scott, Prof. S.-H. Lee
Department of Mechanical Engineering
University of Colorado at Boulder
Boulder, CO 80309-0215, USA
Dr. A. S. Cavanagh, N. E. Widjonarko
Department of Physics
University of Colorado at Boulder
Boulder, CO 80309-0215, USA
Prof. S. M. George
Department of Chemistry and Biochemistry
University of Colorado at Boulder
Boulder, CO 80309-0215, USA
Prof. S. M. George
Department of Chemical and Biological Engineering
University of Colorado at Boulder
Boulder, CO 80309-0215, USA

DOI: 10.1002/aenm.201100750

vehicular applications. For example, the inorganic–polymer composite separators require a completely new manufacturing process compared to that of conventional pure-polymer separators. In the case of the inorganic/polymer/inorganic trilayer separators, the appreciable gain in film thickness will lead to a decrease in energy density (in a full battery). Furthermore, the polymer layer itself between two inorganic layers may still have wetting issues.

Our group has demonstrated that atomic layer deposition (ALD) is a very promising coating technology to tailor various cathodes (bulk-$LiCoO_2$ [LCO],[16] nano-$LiCoO_2$[17], nano-$LiNi_{1/3}Mn_{1/3}Co_{1/3}O_2$[18]) and anodes (graphite,[19] MoO_3,[20] Fe_3O_4[21]) for improved LIB durability, safety, and rate performance. ALD is based on sequential and self-limiting surface reactions.[22] As an example, the reaction sequences of an ALD process to deposit one atomic layer of Al_2O_3 utilizing trimethylaluminium (TMA) and H_2O as precursors are shown below:[22,23]

$$AlOH^* + Al(CH_3)_3 \rightarrow AlO - Al(CH_3)_2^* + CH_4 \quad (1)$$

$$AlCH_3^* + H_2O \rightarrow Al - OH^* + CH_4 \quad (2)$$

The self-limiting reactions in the ALD process produce a conformal film and allow for precise control of atomic thickness. Importantly, the vapor-phase ALD precursors can access a tortuous porous network, such as conventional composite electrodes, and are deposited on all exposed surfaces.[19] Al_2O_3 ALD has been previously employed on polymer substrates by absorbing TMA within the porous polymer surfaces.[24,25] Inspired by this work, we report on thin ALD Al_2O_3-coated porous PP separators (Celgard 2500). An Al_2O_3 layer less than ~10 nm is coated on every surface of the porous polymer microframework without significantly increasing the separator thickness, as depicted by the schematic in **Scheme 1**a. In contrast, the thickness of a conventional "trilayer" ceramic-coated polymer separator is increased substantially (Scheme 1b). Importantly, the thin Al_2O_3 ALD coating enables not only significantly suppressed thermal shrinkage, but also excellent wettability even with an extremely polar electrolyte where pure PC is used as the solvent.

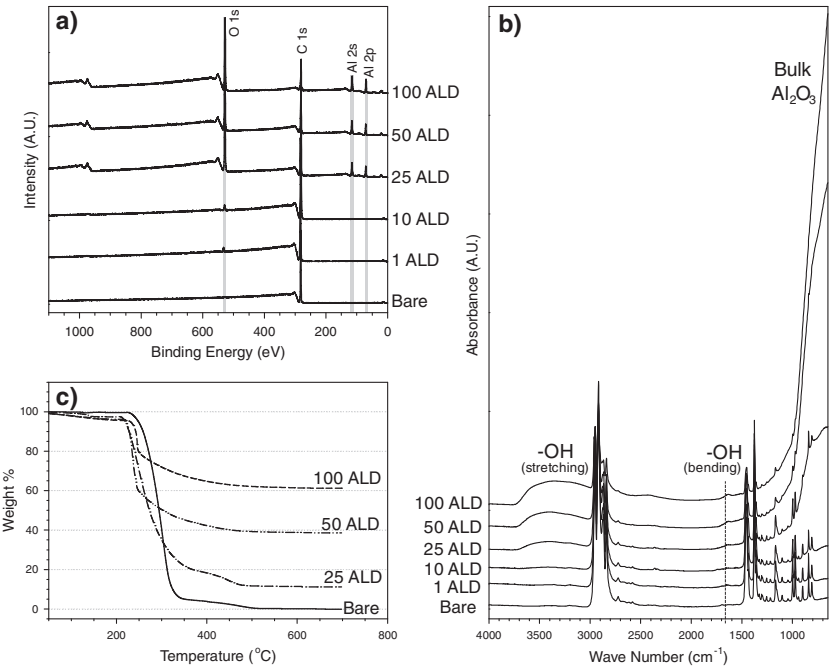

Figure 1. a) XPS spectra, b) TGA profiles (in air), and c) FTIR spectra of bare and Al_2O_3 ALD-coated separators. ALD cycle numbers are indicated.

2. Results and Discussion

The initiation mechanism of ALD on polymers is quite different from that of hydroxyl group (–OH)-terminated inorganic materials.[25] TMA is adsorbed onto the surface, and the near-surface region of the polymer. The adsorbed TMA then reacts with H_2O in the next step.

Al_2O_3-coated PP separators were prepared with 1, 10, 25, 50, and 100 cycles of ALD. X-ray photoelectron spectroscopy (XPS) spectra of the samples shown in **Figure 1**a reveal the increasing intensities of Al (Al 2s and 2p) and O (O 1s) with increasing ALD cycle numbers. This observation is consistent with attenuated total reflectance Fourier transform infrared spectroscopy (ATR-FTIR) spectra (Figure 1b and Figure S1, Supporting Information (SI)), where the Al_2O_3 bulk vibrational modes (400–1000 cm^{-1}) are clearly observed.[24] The weight and volume fractions of Al_2O_3 in the Al_2O_3 ALD-coated separators derived from thermogravimetric analysis (TGA) (Figure 1c) are also provided in **Table 1**. Importantly, the Al_2O_3 ALD-coated separators do not lose their excellent flexibility, as depicted by the photographs in Figure S2 (SI), and the coated separators are easily bent.

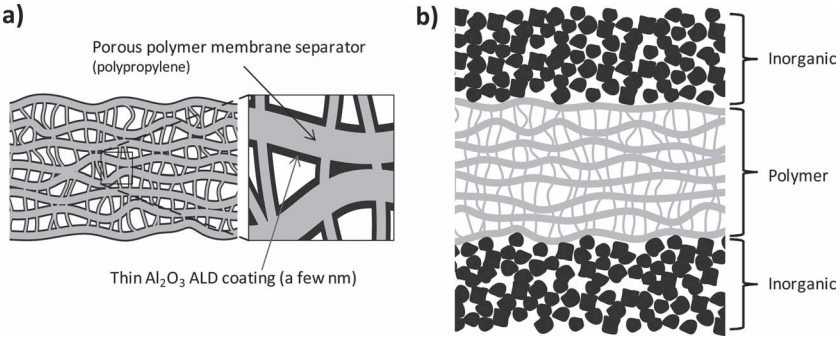

Scheme 1. Schematic cross-sectional diagram of a) ALD-coated porous polymer membrane separator, where a thin Al_2O_3 layer (a few nm) is conformally coated on the porous microstructure, and b) conventional ceramic-coated inorganic/polymer/inorganic trilayer film separator.

Table 1. Fraction of Al_2O_3 and porosity of Al_2O_3 ALD-coated separators derived from TGA.

ALD cycle number	Fraction of Al_2O_3 ALD		Porosity [%][a)]
	Weight [%]	Volume [%][a)]	
Bare	0	0	55
25 ALD	11.5	4.3	53
50 ALD	40.1	18.6	44
100 ALD	64.0	37.8	26

[a)]Derivation of volume fraction of Al_2O_3 and porosity is described in SI.

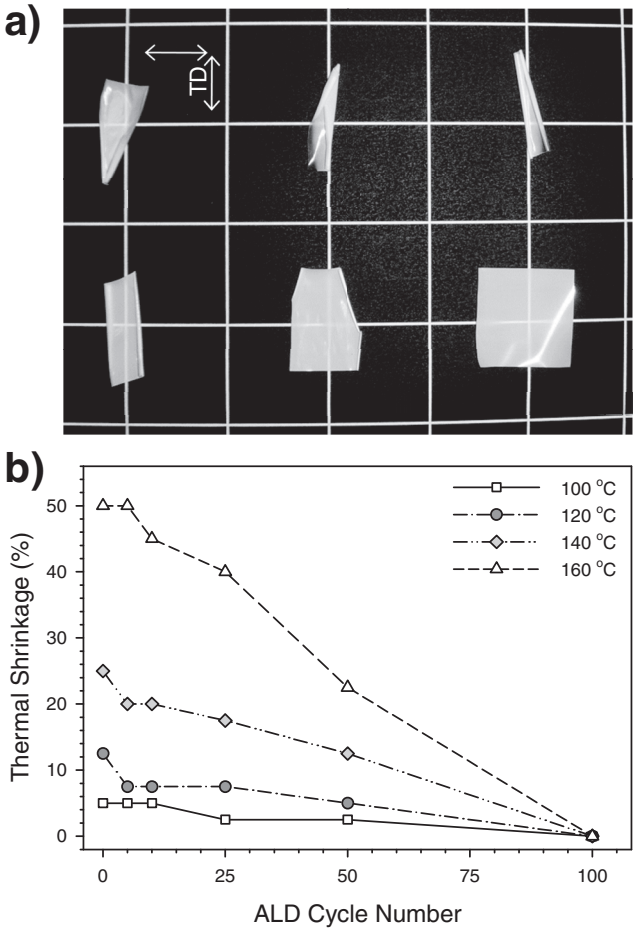

Figure 3. Thermal shrinkage of bare and Al_2O_3 ALD-coated separators. a) Photographic images of bare and Al_2O_3 ALD-coated separators after exposure to 160 °C for 30 min. One grid corresponds to 2 cm and b) a summary of thermal shrinkage as a function of ALD cycle number and temperature. Shrinkage occurs only in the MD (MD and TD indicated in (a)).

Figure 2a shows an even distribution of Al and O signals detected with energy dispersive spectroscopy (EDS) in a field emission scanning electron microscopy (FESEM) image of the Al_2O_3-coated separator following 50 ALD cycles. More importantly, an even distribution of Al and O is observed throughout the entire film, as shown by EDS and FESEM in cross-sectional views of the coated separator in Figure 2b. This confirms that the ALD precursors (TMA and H_2O) diffuse through the tortuous PP network and are deposited in the inner surfaces similar to our previous work on ALD-coated as-fabricated porous composite electrodes.[19] As depicted in the cross-sectional FESEM images of the bare separator (Figure 2c) and the Al_2O_3 ALD-coated separators after 50 and 100 ALD cycles (Figure 2d,e), the overall thickness of the film does not change after ALD coating. This is an important advantage of ALD coatings compared with conventional inorganic/polymer/inorganic trilayer separators.[12–15] Also, as shown in the FESEM image in Figure 2c, the bare PP separator has slit-like pores of ~500 nm in length and ~50 nm in width, consistent with previous reports.[4,26] Because the Al_2O_3 growth rate on PP is expected to be ~1.2 Å per cycle,[25] 50 ALD cycles result in an ~6 nm layer film. This should not significantly affect the pore structure, as the limiting dimension above is ~50 nm. This is confirmed by the FESEM image in Figure 2d, where the original pores are still visible. However, after 100 ALD cycles, the pores in Figure 2e seem to disappear. Theoretically, pores with widths of ~50 nm should allow for an ALD coating of ~12 nm. However, the conductive Au/Pd coating employed for preparation of the FESEM sample may contribute to the pores disappearing (Figure 2e). Assuming that approximate values for the ALD coating and Au/Pd layer may be expressed by: (12 nm × 2, Al_2O_3) + (17 nm × 2 AuPd) = 58 nm, it is possible to explain the relatively poreless features in Figure 2e, but to still assume that the pores are open even after 100 ALD cycles. Porosity information for the Al_2O_3 ALD-coated separators is also derived from TGA (Table 1). After 50 ALD cycles, the porosity has not decreased significantly (Bare: 55%, 50 ALD

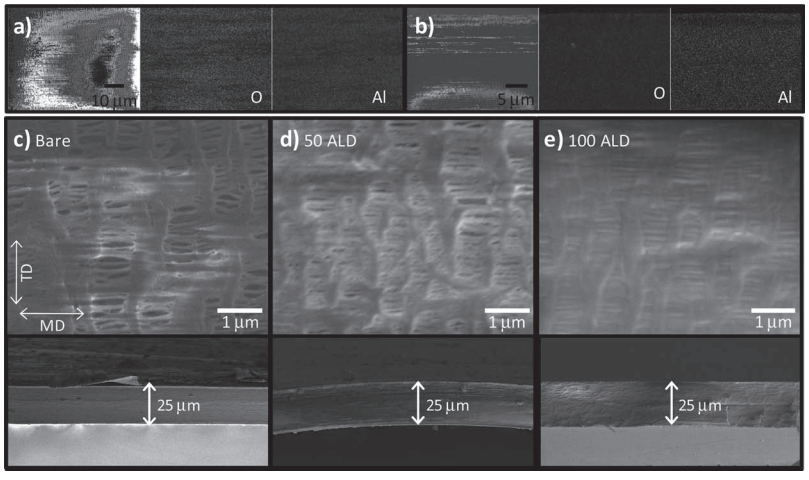

Figure 2. FESEM images of a) top and b) cross-sectional views and their corresponding EDS maps (O and Al) of Al_2O_3-coated separators with 50 ALD cycles. FESEM images of top (upper) and cross-sectional (lower) views of c) bare separator and Al_2O_3-coated separators with d) 50 and e) 100 ALD cycles. Machine direction (MD) and transverse direction (TD) are indicated in (c).

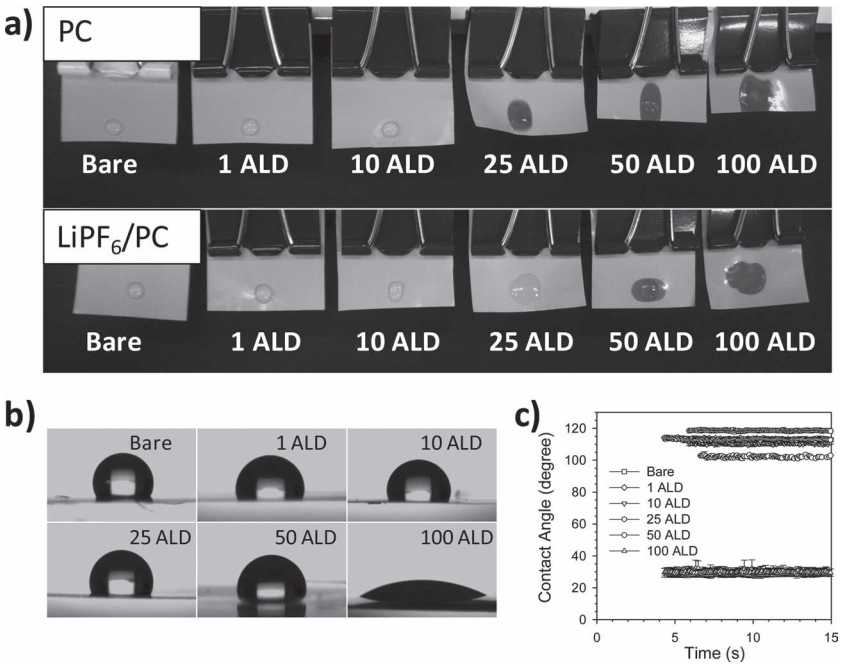

Figure 4. a) Photographs of bare and Al_2O_3 ALD-coated separators contacted with PC and 1 M $LiPF_6$ in pure PC. b) Contact angle images of bare and Al_2O_3 ALD-coated separators with water, and c) their extracted values as a function of time.

cycles: 44%). However, although the porosity is decreased to 26% after 100 ALD cycles, this still indicates that the Al_2O_3 coating does not completely fill the pore volumes. We also note that the TGA numbers are consistent with simply calculating the narrowing of the pores by the anticipated ALD-coating thickness, which will be further discussed below.

Thermal shrinkage was measured by keeping 2 cm × 2 cm separators inside a preheated oven at designated temperatures for 30 min. Shrinkage takes place in only one direction (machine direction [MD]), as demonstrated in a previous report.[4] **Figure 3**a shows photographic images of a bare separator and separators coated with various cycles of ALD after maintaining the separators at 160 °C. Surprisingly, after 100 ALD cycles, the coated membrane retains its original dimensions. Figure 3b summarizes the results, and two trends are clear. First, as the temperature increases from 100 to 160 °C, shrinkage becomes more severe. Second, shrinkage is significantly suppressed with increasing ALD cycle numbers. Notably, 100 ALD cycles results in no shrinkage at all. This significantly suppressed thermal shrinkage may lead to greatly improved safety of the battery.[4] The conformal Al_2O_3 ALD coating is believed to help maintain the mechanical integrity of the polymer framework. This phenomenon is surprising in that the coating layer does not exceed ~12 nm, but results in dramatic improvement to the mechanical properties, which may be in line with the unusually improved mechanical properties encountered in organic/inorganic hybrid materials.[27]

The Al_2O_3 ALD coating changes the polymer surface property as the Al_2O_3 surface is terminated by hydrophilic Al–OH groups. Significantly increasing intensities of the broad peaks from –OH stretching (3700–3000 cm^{-1}) and bending (1640 cm^{-1}) vibrational modes in ATR FTIR spectra with increasing ALD cycle numbers (Figure 1c) are attributed to the increased adsorption of water on the –OH terminated Al_2O_3 surfaces.[28] Accordingly, the wettability with an extremely polar solvent (pure PC) and electrolyte (1 M $LiPF_6$ in pure PC) is dramatically enhanced by increasing ALD cycle numbers as demonstrated by the photographs in **Figure 4**a. Complete wetting is clearly observed after 25 and 50 ALD cycles for both pure PC and $LiPF_6$ in pure PC, respectively. Contact angle measurements with water also agree well with this observation. In that, the contact angle of water decreases with increasing ALD cycle numbers (Figure 4b,c).

The electrochemical performance of Al_2O_3 ALD-coated separators is characterized by cycling nano-$Li_4Ti_5O_{12}$ (LTO, anode)/$LiFePO_4$ (LFP, cathode) full cells between 1.0 and 2.5 V at room temperature. These nanostructured electrodes were chosen because the electrodes themselves can exhibit high-rate performance due to short diffusion length. With a conventional electrolyte (1 M $LiPF_6$ in a conventional mixture of EC and diethyl carbonate [DEC]), the high-rate performance does not degrade after 25 or 50 ALD cycles on the separator, as shown in **Figure 5**a. This indicates that the slightly decreased pore size by up to 50 ALD cycles (~6 nm) does not reduce the rate capability of LTO/LFP full cells, and that Li^+-ion diffusion in solids or charge transfer resistance is more critical. As depicted by the voltage profiles in Figure 5b, of the coated and bare separators, the polarization increase after 50 ALD cycles is negligible at rates of 1C, 10C, and 40C. However, 100 ALD cycles leads to decreased capacities at higher rates (Figure 5a), which is attributed to the significantly narrowed pores by the thicker Al_2O_3 coating (~10–12 nm). Similarly, long-term cycling stability after 25 and 50 ALD cycles is demonstrated to be nearly identical to the cell with a bare separator (~96% capacity retention at 4C after 1000 charge–discharge cycles, Figure 5c). This result agrees well with the FESEM and TGA results, where the pore structure or porosity is not significantly altered with up to 50 ALD cycles.

The performance of the cells using the extremely polar electrolyte (1 M $LiPF_6$ in pure PC) is displayed in **Figure 6**. Employing, this polar electrolyte for the cell with a bare separator did not result in reversible cycling (not shown). However, the cell containing the 50 ALD-coated separator using $LiPF_6$ in PC (Figure 6a) exhibited almost the same high-rate performance as the cell with a bare separator and the conventional electrolyte, (1 M $LiPF_6$ EC/DEC) (Figure 5a). Also, the cell with 50 ALD cycles using $LiPF_6$ in pure PC exhibited reasonable cycling stability (~80% capacity retention at 4C after 1000 charge–discharge cycles, Figure 6b). Collectively, these results show that by employing the Al_2O_3 ALD-coated separators, wetting issues are solved and good ion conductivity is still maintained. Thus, choices in the electrolyte systems may then be unprecedentedly broadened. The poor cycling performance at different rates with 25 and 100 ALD cycles using $LiPF_6$ in PC (Figure 4c) are

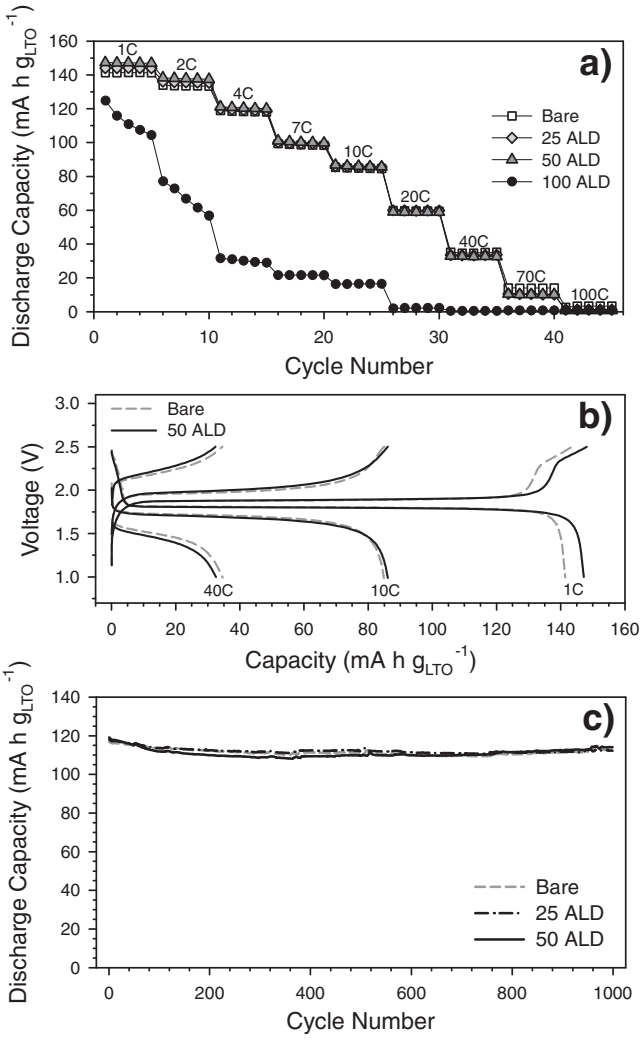

Figure 5. Electrochemical performance of LTO/LFP full cells in 1 M $LiPF_6$ in a mixture of EC and DEC using bare and Al_2O_3 ALD-coated separators. a) Cycling data with variable rates, b) charge–discharge voltage profiles, and c) cycling performance at 4C.

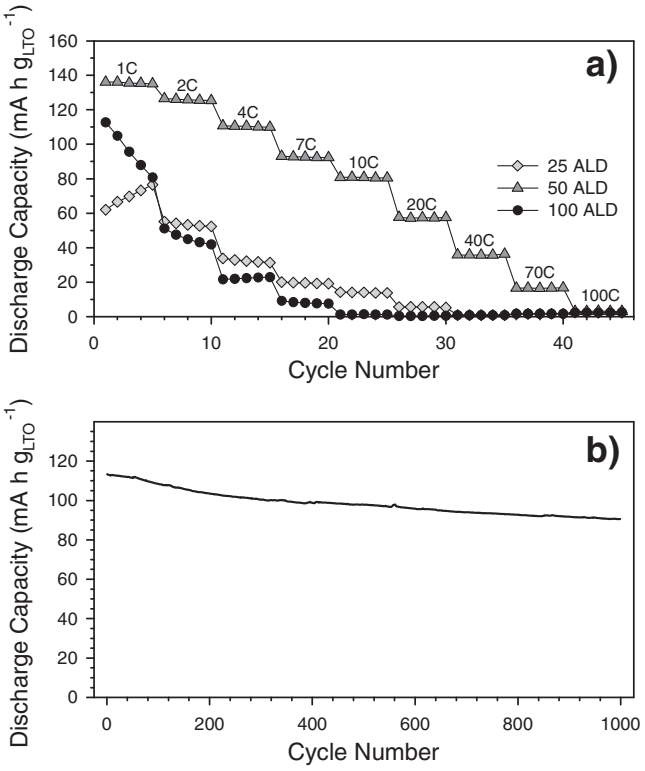

Figure 6. Electrochemical performance of LTO/LFP full cells in 1 M $LiPF_6$ in pure PC using Al_2O_3 ALD-coated separators. a) Cycling data with variable rates with Al_2O_3-coated separators following 25, 50, and 100 ALD cycles. b) Cycling performance with an Al_2O_3-coated separator following 50 ALD cycles. The cells were cycled between 1.0 and 2.5 V at 4C.

attributed to not enough hydrophilicity and too-narrow pores, respectively. Thus, 50 ALD cycles is optimal for the coated PP separator in a polar electrolyte without losing high-rate capability. To our knowledge, there is no report where the electrolyte is comprised of pure PC and employed with polymer-based separators. Even though the inorganic layers, for the case of inorganic/polymer/inorganic trilayer separators, can help to absorb and transport the polar electrolyte, it still remains uncertain whether the sandwiched polymer layer is completely wetted by extremely polar electrolytes.

As a further proof of concept, a LCO/natural graphite (NG) full cell, where both the two electrodes and the separator are coated with Al_2O_3 ALD, was cycled between 3.25 and 4.45 V at 0.1C (140 mA g_{LCO}^{-1}) for the first two cycles and 1C for subsequent cycles. The LCO/NG cycled between 3.25 and 4.45 V using $LiPF_6$ in pure PC will not cycle reversibly without an Al_2O_3 ALD coating on all three components for three reasons: 1) the LCO degrades very quickly at high potential (>4.2 V [versus Li/Li^+]),[16,17] 2) a permanent decomposition reaction of PC occurs on NG[19], and 3) the conventional polyolefin separators are not wetted by $LiPF_6$ in the pure PC electrolyte, consistent with Figure 4a. Importantly, the coated separator enables the use of PC due to improved wettability, and by also coating the NG anode, we have demonstrated that it is possible to cycle graphite in PC. By applying an Al_2O_3 ALD coating to the LCO, NG, and separator, the cell shows stable cycling performance (with 82% capacity retention after 150 cycles compared with the capacity at the third cycle, **Figure 7**). This demonstrates the promise of ALD coatings for LIBs to enable surface protection on the cathode and anode, as well as wettability of the separator with polar electrolytes.

3. Conclusion

A thin ALD Al_2O_3 layer (~6 nm) was applied to the porous microstructure of PP separators without an overall increase in the total separator thickness. The thin Al_2O_3 ALD coating enabled significantly improved safety due to suppressed thermal shrinkage. More importantly, wettability in the extremely polar PC-based electrolyte was demonstrated without a decrease in electrochemical performance. By coating NG, we also have demonstrated that it does not degrade in PC. Thus, we believe that these results are important to the development of high-performance LIBs for electric vehicles.

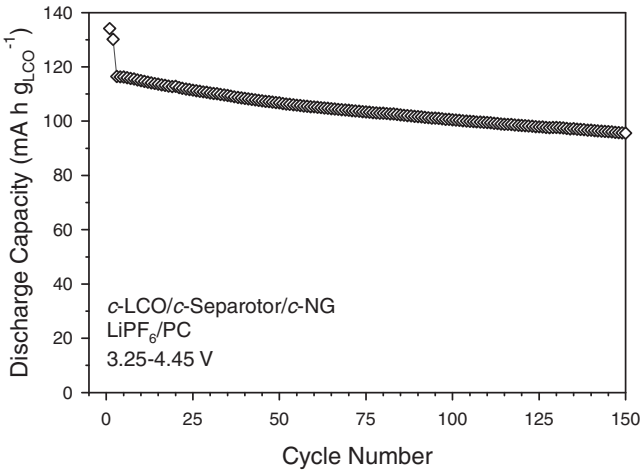

Figure 7. Cycling performance of Al_2O_3 ALD-coated LCO/NG cell cycled using 1 M $LiPF_6$ in pure PC between 3.25 and 4.45 V at 0.1C for the first two cycles and 1C for the subsequent cycles. The cathode (LCO), anode (NG), and separator were coated by Al_2O_3 with 2 ALD cycles, 5 ALD cycles with TMA/NO_2 pretreatment, and 50 ALD cycles, respectively. The ALD was applied directly on as-fabricated electrodes (LCO and NG) as described in previous work.

4. Experimental Section

Al_2O_3 ALD on a Porous PP Separator: Al_2O_3 ALD films were grown on a porous PP separator (Celgard 2500) at 50 °C using a rotary ALD reactor. Detailed ALD reaction sequences have been described in previous reports.[16,19]

Materials Characterization: A PHI 5600 X-ray photoelectron spectrometer was employed to obtain XPS of the samples. Monochromatic Al K X-rays (1486.6 eV) were used for the XPS analyses. FESEM images were obtained using a FEI Nova NanoSEM 630 FESEM. EDS mapping analyses were carried out using an EDAX Apollo SDD. The samples for FESEM and EDS were coated with approximately 17 nm Au/Pd by sputtering at 35 mA for 25 s. The TGA data were obtained from 50 to 700 °C at 5 °C min^{-1} in air with a TA instrument Q 600 TGA analyzer.

Electrochemical Characterization: The LTO and LFP electrodes were prepared by spreading the active materials (LTO powders [MTI corp.]), carbon black (CB) (super C65, TIMCAL Ltd.), and polyvinylidene fluoride (PVDF) (binder, Kynar) (70:15:15) on a pieces of Cu and Al foils for the anode (LTO) and the cathode (LFP), respectively. The electrodes and the separators were dried under vacuum overnight at 120 and 50 °C, respectively. LTO/LFP full cells were assembled as 2032-type coin cells in an Ar-dry box. The mass ratio of LFP/LTO in the full cells was ≈1.4–1.5. The overall capacity of the full cell is limited by the capacity of the LTO. The conventional electrolyte was purchased from Novolyte Technologies, Inc. (1.0 M $LiPF_6$ dissolved in a mixture of EC and DEC [1:1 v/v]). Another electrolyte was prepared by dissolving 1.0 M $LiPF_6$ (Alfa Aesar) in pure anhydrous PC (Sigma–Aldrich) in an Ar-dry box. The galvanostatic charge–discharge cycling tests of the LTO/LFP cells were performed between 1.0 and 2.5 V at various C rates at room temperature. One C rate corresponds to 160 mA g_{LTO}^{-1}. The NG/LCO full cells were similarly prepared.

Supporting Information

Supporting Information is available from the Wiley Online Library or from the author.

Acknowledgements

This research was funded by the US Department of Energy under Contract No. DE-AC36-08-GO28308 through the National Renewable Energy Laboratory's Laboratory Directed Research and Development Program. This work was also supported by Energy Efficiency and Resources R&D program (20112010100150) under the Ministry of Knowledge Economy, Republic of Korea, and by the year of 2011 Research Fund of the UNIST (Ulsan National Institute of Science and Technology). The authors thank Bobby To for FESEM images and EDS maps, and Katherine Hurst and Joel Pankow for assisting with TGA measurements, and contact angle measurements, respectively.

Received: December 12, 2011
Revised: February 10, 2012
Published online: April 27, 2012

[1] M. Armand, J.-M. Tarascon, *Nature* **2008**, *451*, 652.
[2] J. B. Goodenough, Y. Kim, *Chem. Mater.* **2010**, *22*, 587.
[3] A. C. Dillon, *Chem. Rev.* **2010**, *110*, 6856.
[4] P. Arora, Z. Zhang, *Chem. Rev.* **2004**, *104*, 4419.
[5] S. Tobishima, J. Yamaki, *J. Power Sources* **1999**, *81*, 882.
[6] D.-W. Kim, J.-M. Ko, J.-H. Chun, S.-H. Kim, J.-K. Park, *Electrochem. Commun.* **2001**, *3*, 535.
[7] J. M. Ko, B. G. Min, D.-W. Kim, K. S. Ryu, K. M. Kim, Y. G. Lee, S. H. Chang, *Electrochim. Acta* **2004**, *50*, 367.
[8] Y.-B. Jeong, D.-W. Kim, *J. Power Sources* **2004**, *128*, 256.
[9] M.-H. Ryou, Y. M. Lee, J.-K. Park, J. W. Choi, *Adv. Mater.* **2011**, *23*, 3066.
[10] S. S. Zhang, K. Xu, T. R. Jow, *J. Power Sources* **2005**, *140*, 361.
[11] D. Takemura, S. Aihara, K. Hamano, M. Kise, T. Nishimura, H. Urushibata, H. Yoshiyasu, *J. Power Sources* **2005**, *146*, 779.
[12] J. Y. Kim, S. K. Kim, S.-J. Lee, S. Y. Lee, H. M. Lee, S. Ahn, *Electrochim. Acta* **2004**, *50*, 363.
[13] S. Augustin, V. D. Hennige, G. HÖrpel, C. Hying, J. Tarabocchia, J. Swoyer, M. Y. Saïdi, *208th ECS Meeting*, Los Angeles, CA **2005**, Abstract #80.
[14] J.-A. Choi, S. H. Kim, D.-W. Kim, *J. Power Sources* **2010**, *195*, 6192.
[15] M. Kim, G. Y. Han, K. J. Yoon, J. H. Park, *J. Power Sources* **2010**, *195*, 8302.
[16] Y. S. Jung, A. S. Cavanagh, A. C. Dillon, M. D. Groner, S. M. George, S. H. Lee, *J. Electrochem. Soc.* **2010**, *157*, A75.
[17] I. D. Scott, Y. S. Jung, A. S. Cavanagh, Y. Yan, A. C. Dillon, S. M. George, S.-H. Lee, *Nano Lett.* **2011**, *11*, 414.
[18] L. A. Riley, S. Van Ana, A. S. Cavanagh, Y. Yan, S. M. George, P. Liu, A. C. Dillon, S.-H. Lee, *J. Power Sources* **2010**, *196*, 3317.
[19] Y. S. Jung, A. S. Cavanagh, L. A. Riley, S. H. Kang, A. C. Dillon, M. D. Groner, S. M. George, S. H. Lee, *Adv. Mater.* **2010**, *22*, 2172.
[20] L. A. Riley, A. S. Cavanagh, S. M. George, Y. S. Jung, Y. Yan, S. H. Lee, A. C. Dillon, *ChemPhysChem* **2010**, *11*, 2124.
[21] E. Kang, Y. S. Jung, A. S. Cavanagh, G.-H. Kim, S. M. George, A. C. Dillon, J. K. Kim, J. Lee, *Adv. Funct. Mater.* **2011**, *21*, 2430.
[22] S. M. George, *Chem. Rev.* **2010**, *110*, 111.
[23] A. C. Dillon, A. W. Ott, J. D. Way, S. M. George, *Surf. Sci.* **1995**, *322*, 230.
[24] J. D. Ferguson, A. W. Weimer, S. M. George, *Chem. Mater.* **2004**, *16*, 5602.
[25] C. A. Wilson, R. K. Grubbs, S. M. George, *Chem. Mater.* **2005**, *17*, 5625.
[26] T. Sarada, L. C. Sawyer, M. I. Ostler, *J. Membrane Sci.* **1983**, *15*, 97.
[27] S.-M. Lee, E. Pippel, U. Gösele, C. Dresbach, Y. Qin, C. V. Chandran, T. Bräuniger, G. Hause, M. Knez, *Science* **2009**, *324*, 488.
[28] H. A. Al-Abadleh, V. H. Grassian, *Langmuir* **2003**, *19*, 341.